Stable Ta_2O_5 overlayers on α-Fe_2O_3 photoelectrodes for water splitting

Mark Forster,[a] Richard J. Potter,[b] Yichuan Ling,[c] Yi Yang,[c] Yat Li[c]
and Alexander J. Cowan[a]*

Electronic supplementary information

Contents

1 Additional information

1.1 Approximate band gaps of α-Fe_2O_3 and Ta_2O_5 along with Al_2O_3 for comparison.

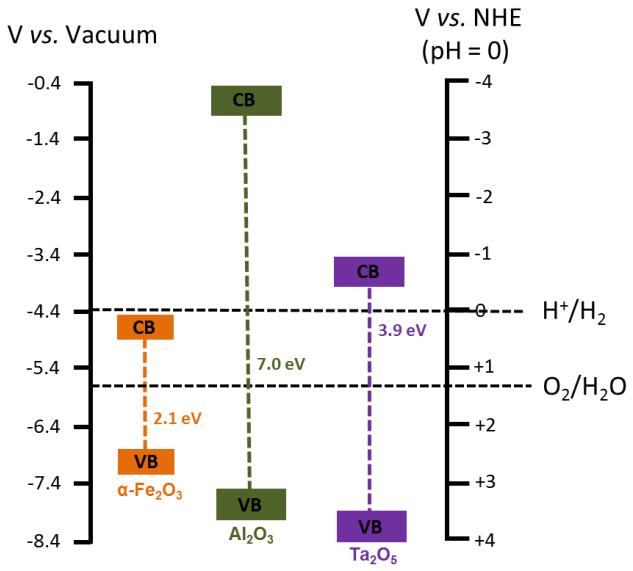

Figure S1. *Approximate valance and conduction band positions based on literature values of α-Fe_2O_3[1], Al_2O_3[2],[3] and Ta_2O_5[4,5].*

1.2 Stability of Ta_2O_5 deposited onto a silicon wafer

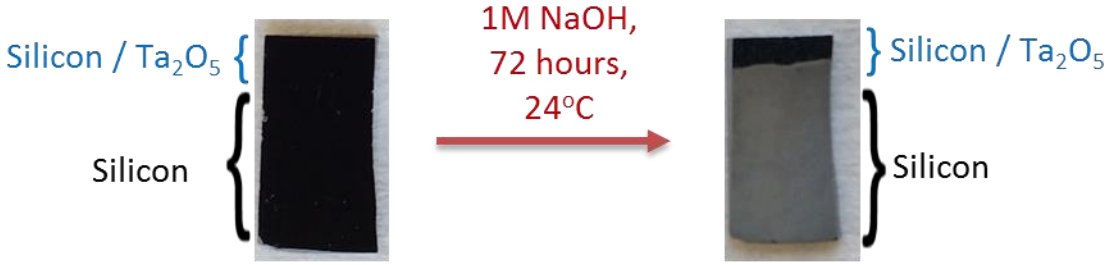

Figure S2. *A silicon wafer partially coated in ~20 nm of Ta_2O_5 before and after being immersed in 1 M NaOH (pH ~13.7) for 72 hours at room temperature (24 °C). The silicon wafer is preserved under the Ta_2O_5 layer while the uncoated region is etched.*

1.3 SEM images of Ta_2O_5 etching on silicon wafer

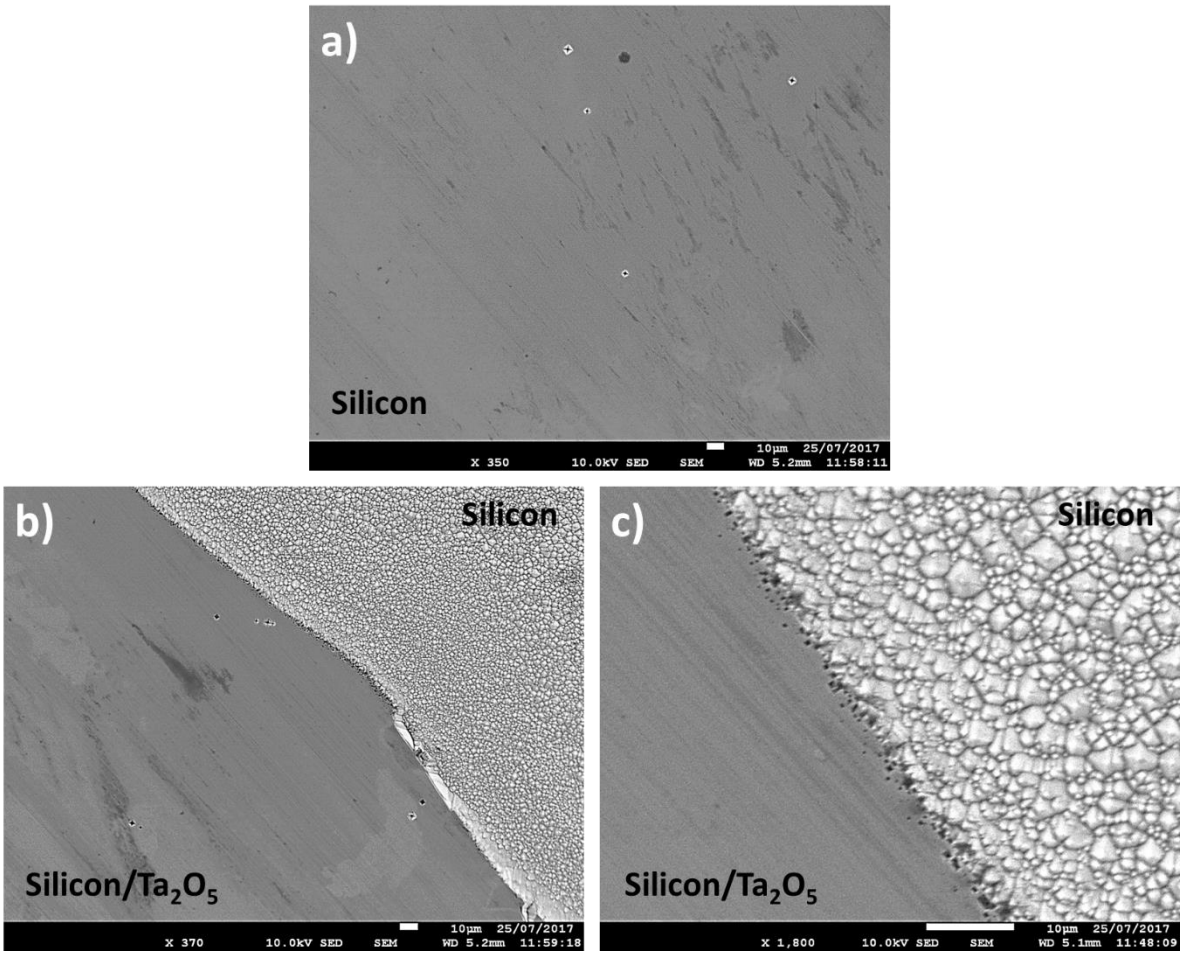

Figure S3. *SEM images of a) a silicon wafer before immersion in 1M NaOH, and b, c) a silicon wafer which has been half coated with a ~20 nm Ta_2O_5 overlayer and immersed in 1M NaOH (pH ~13.7) for 72 hours at room temperature (24 ºC). The silicon wafer is significantly etched by NaOH while the Ta_2O_5 protected part of the wafer remains undamaged.*

1.4 Etching study of Al_2O_3 in 1M NaOH

The etching study of Ta_2O_5 (main text, Figure 2) was also carried out on Al_2O_3 for comparison to an overlayer commonly used for hematite.

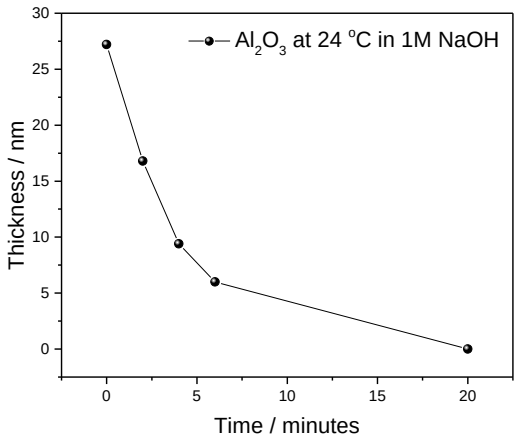

Figure S4. *Thickness of Al_2O_3 with respect to time immersed in 1 M NaOH (pH ~13.7) at room temperature (24 °C) The Al_2O_3 layer was deposited onto standard silicon wafers and thickness was measured by ellipsometry.*

Al_2O_3 was deposited by thermal ALD using trimethyl-aluminium (TMA) and water in an Oxford Instruments OpAL reactor. The reactor was modified by the addition of a process controlled 'hold' valve between the pump and the process chamber, enabling precursor 'soak' steps. These soak steps were chosen to ensure good film density and to promote conformal coating of the nanostructured hematite surface. A low process temperature of 120 °C was chosen to avoid unintentional modification of the hematite samples. Overlayers were deposited using 10 cycles of ALD with a target thickness of ~1 nm of Al_2O_3, using the following sequence:

{(50 ms TMA Dose)(10 s TMA hold)(10 s purge)(30 ms H_2O)(10 s H_2O hold)(10 s purge)}

The growth rate of the Al_2O_3 overlayer was estimated using a Rudulph Auto EL IV ellipsometer operating at 633 nm using silicon 'witness' samples, confirming that 10 cycles gave approximately 1 nm of Al_2O_3.

1.5 Photoelectrochemical response of Ta_2O_5.

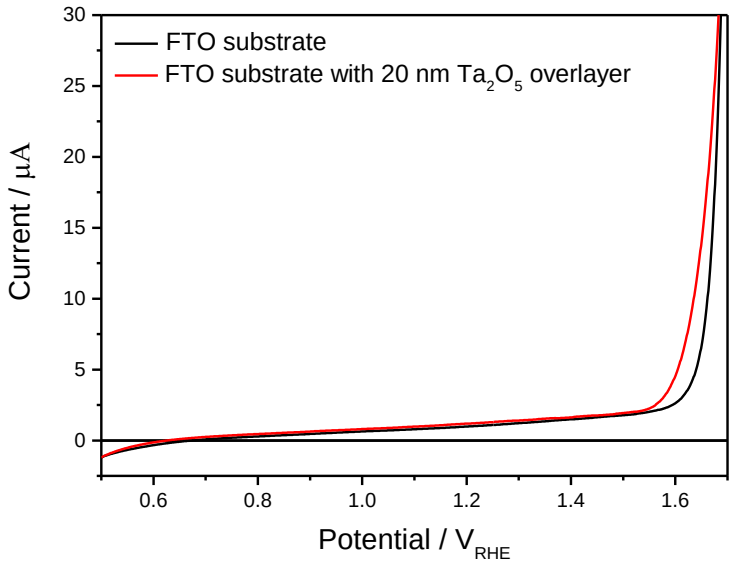

Figure S5. *Linear sweep voltammograms of FTO glass substrate and FTO glass substrate coated with ~20 nm of Ta_2O_5, measured under 50 mW cm^{-2} white light illumination at 10 mV s^{-1} in 1 M NaOH (pH ~13.7).*

1.6 XRD of hematite films with and without Ta_2O_5

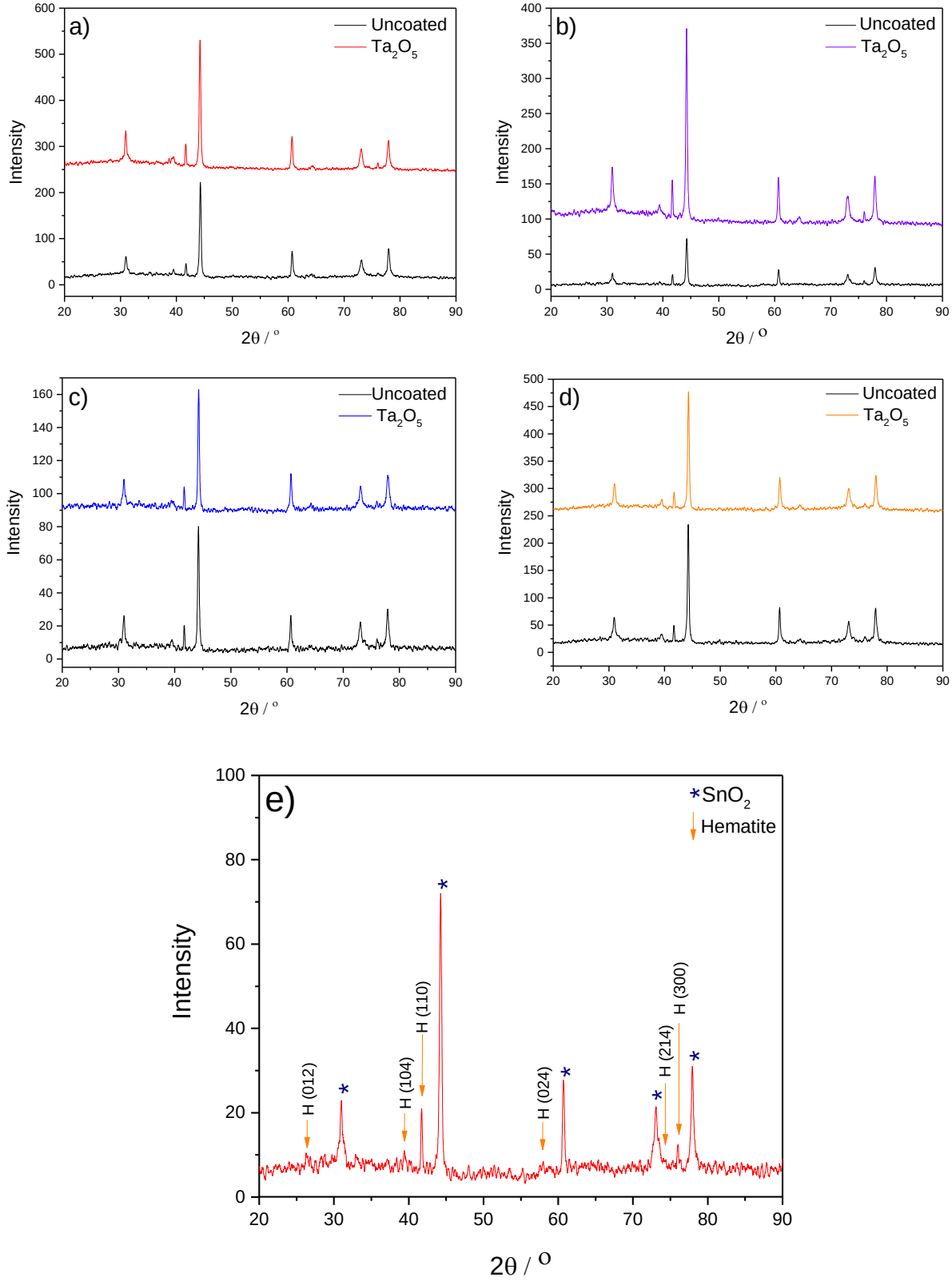

Figure S6. *XRD patterns of (a) 550-Fe_2O_3, b) 750-Fe_2O_3, c) α-Fe_2O_{3-x}, d) α-Fe_2O_3 before and after Ta_2O_5 deposition. e) Shows the assigned peaks for hematite deposited on FTO. The blue stars indicate the peaks assigned to SnO_2 present in the glass substrate and the orange arrows indicate the hematite peaks. Diffraction patterns were recorded on a Panalytical X'Pert PRO HTS X-Ray Diffractometer from 20 to 90° 2 theta with a step size of 0.017 ° at 1.6 ° per minute.*

1.7 UV-Vis absorbance before and after Ta_2O_5 deposition.

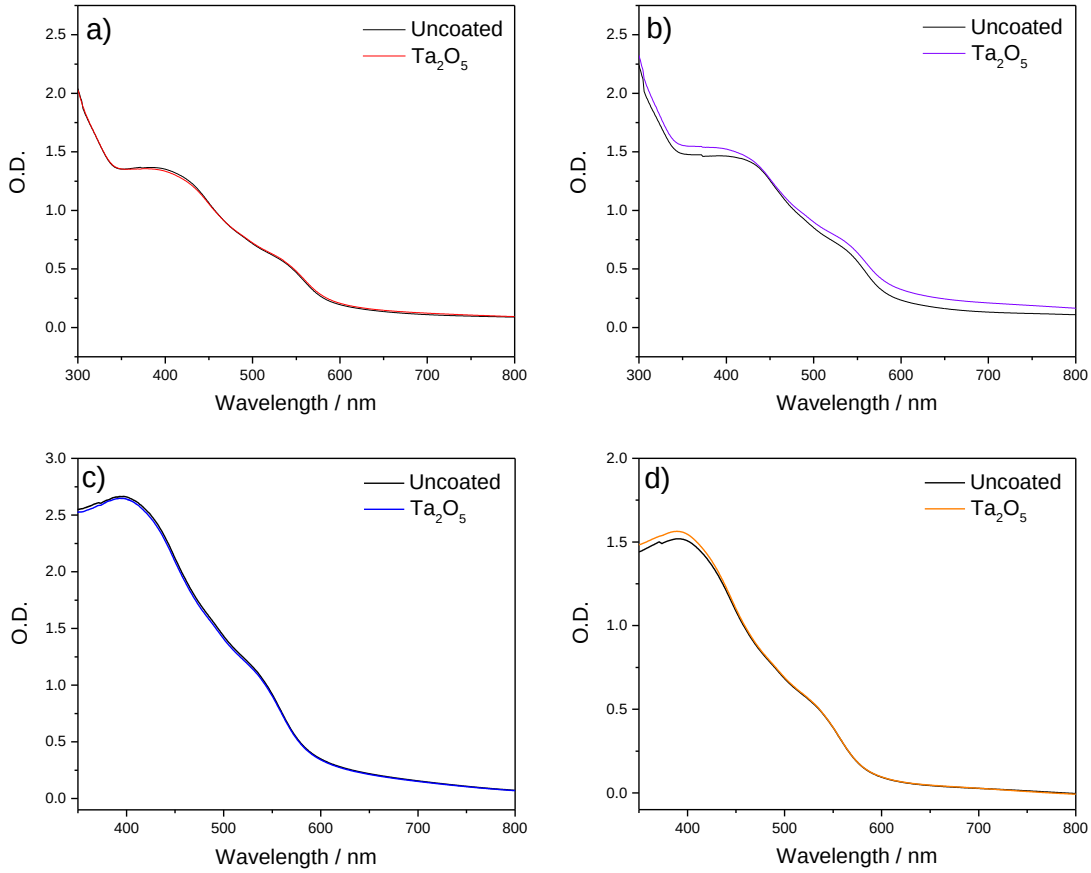

Figure S7. *UV-Vis absorbance spectra of a) 550-Fe_2O_3, b) 750-Fe_2O_3, c) Fe_2O_{3-x} (oxygen deficient) and d) Fe_2O_3 (air annealed), before and after the deposition of a ~2 nm Ta_2O_5 overlayer. Measurements recorded with a Shimadzu UV-2600 spectrophotometer in direct absorbance mode.*

1.8 SEM images before and after Ta_2O_5 deposition.

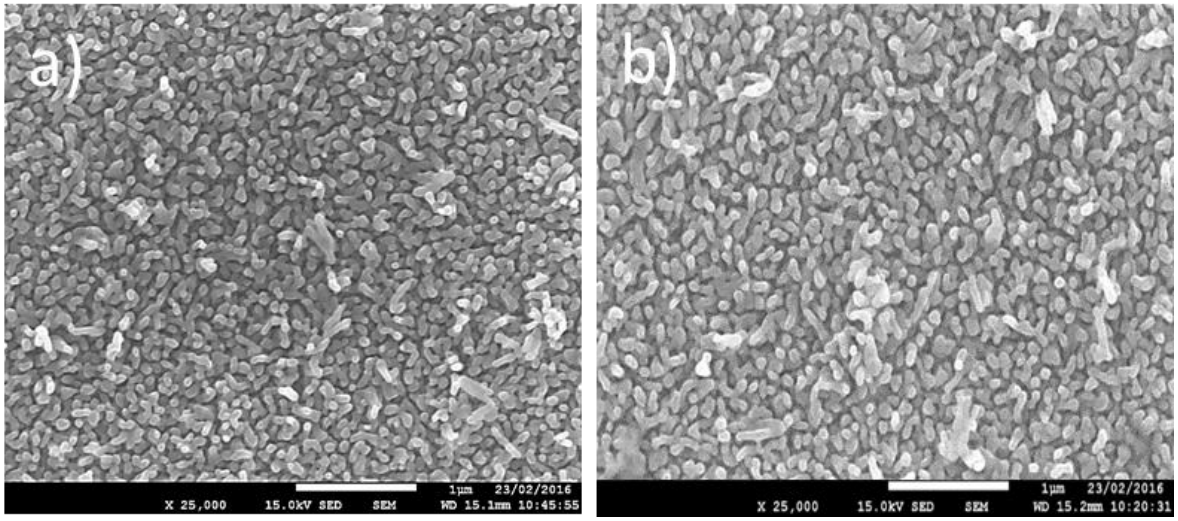

Figure S8. *SEM images of (a) 550- Fe_2O_3 and (b) 550-Fe_2O_3 with a 2 nm Ta_2O_5 overlayer. SEM images were obtained with a Hitachi high resolution 7001 SEM instrument.*

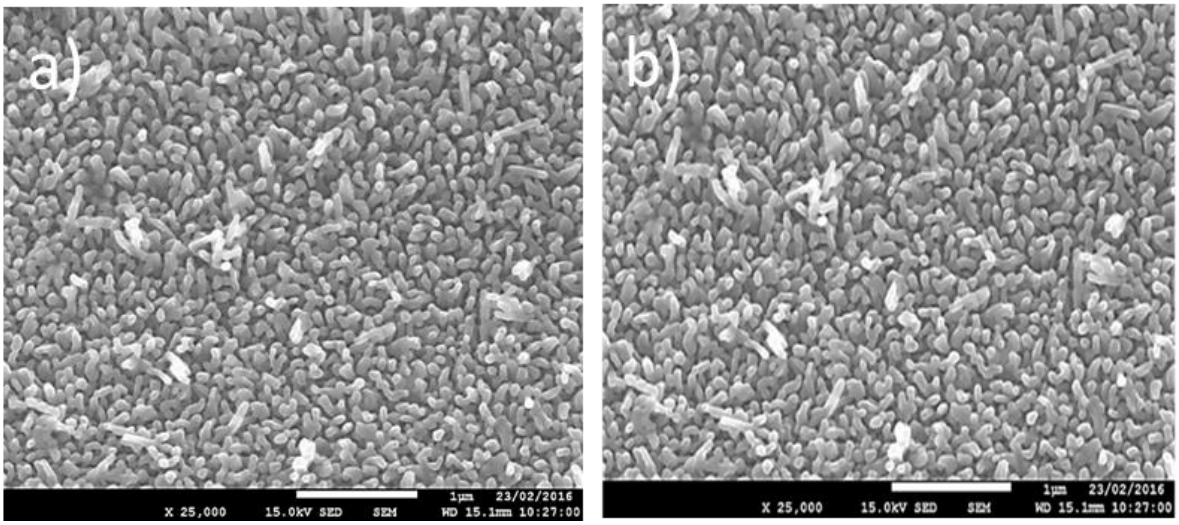

Figure S9. *SEM images of (a) 750- Fe_2O_3 and (b) 750-Fe_2O_3 with a 2 nm Ta_2O_5 overlayer. SEM images were obtained with a Hitachi high resolution 7001 SEM instrument.*

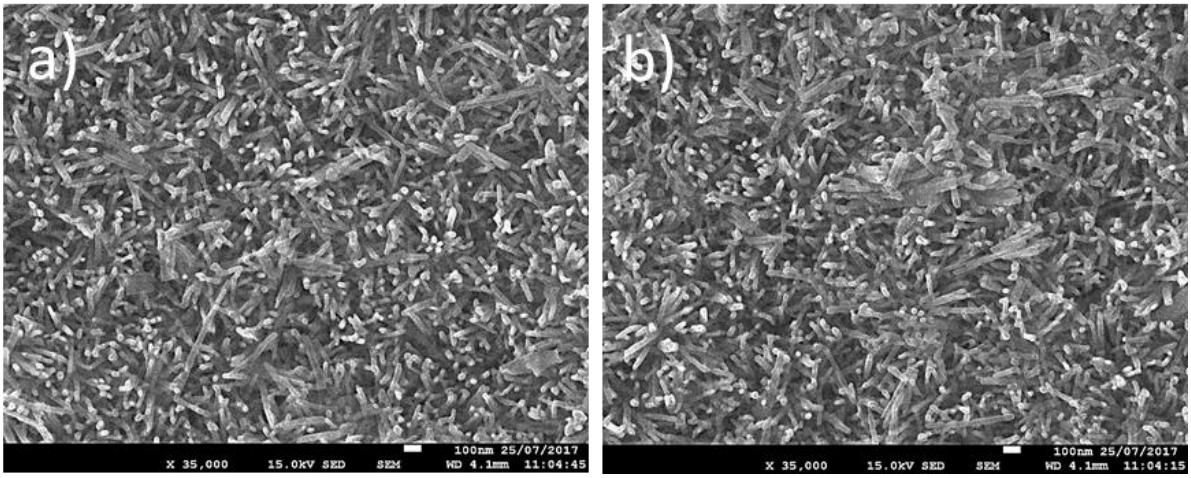

Figure S10. *SEM images of (a) Fe_2O_3 and (b) Fe_2O_3 with a 2 nm Ta_2O_5 overlayer. SEM images were obtained with a Hitachi high resolution 7001 SEM instrument.*

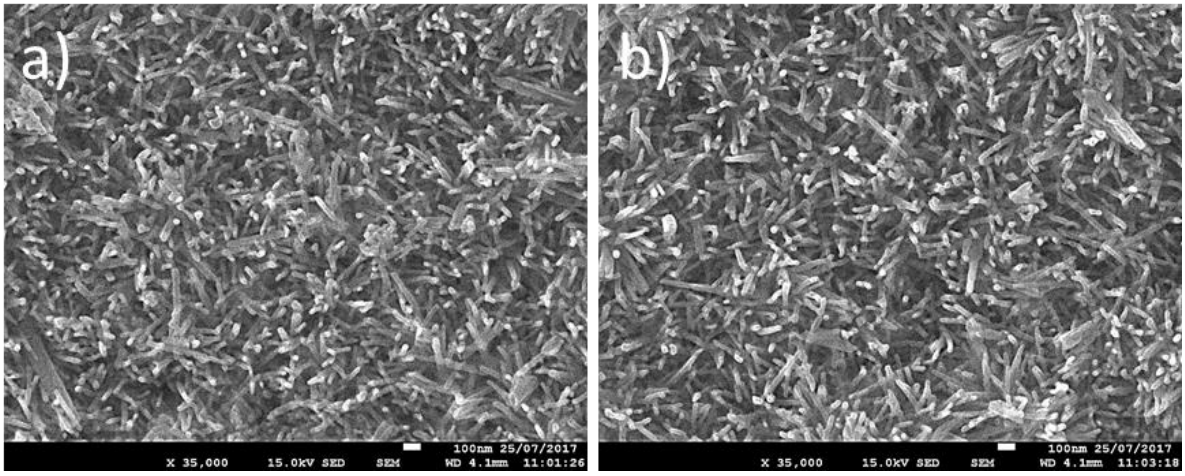

Figure S11. *SEM images of (a) Fe_2O_{3-x} and (b) Fe_2O_{3-x} with a 2 nm Ta_2O_5 overlayer. SEM images were obtained with a Hitachi high resolution 7001 SEM instrument.*

1.9 Heating control experiment at 220 ºC

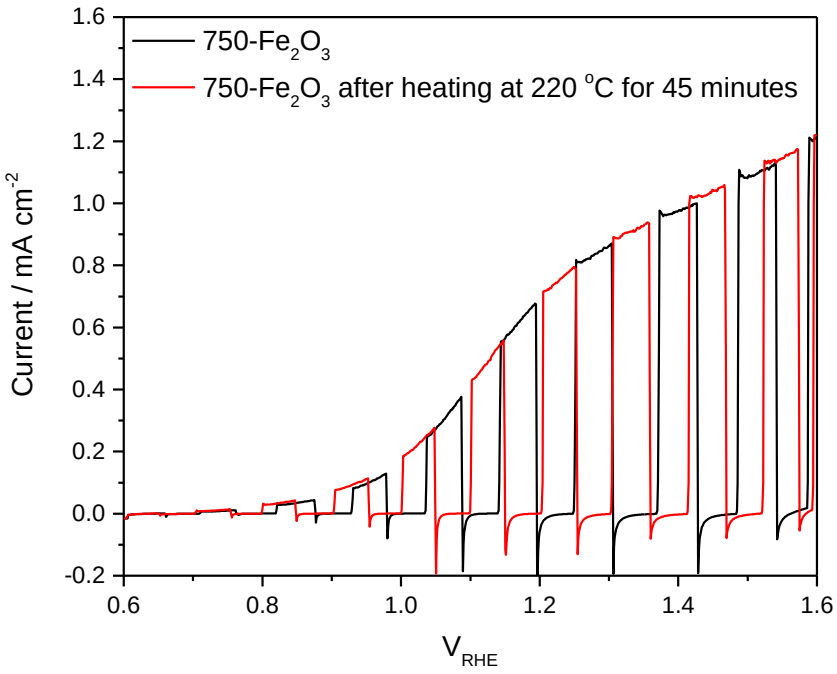

Figure S12. *Chopped light/dark photocurrents of 50-Fe_2O_3, before and after heating at 220 ºC in air for 45 minutes. Scans carried out at 10 mV s^{-1} in the dark and under white light illumination (50 mW cm^{-2}), in 1M NaOH (pH ~13.7).*

1.10 Mott-Schottky before and after Ta_2O_5 deposition.

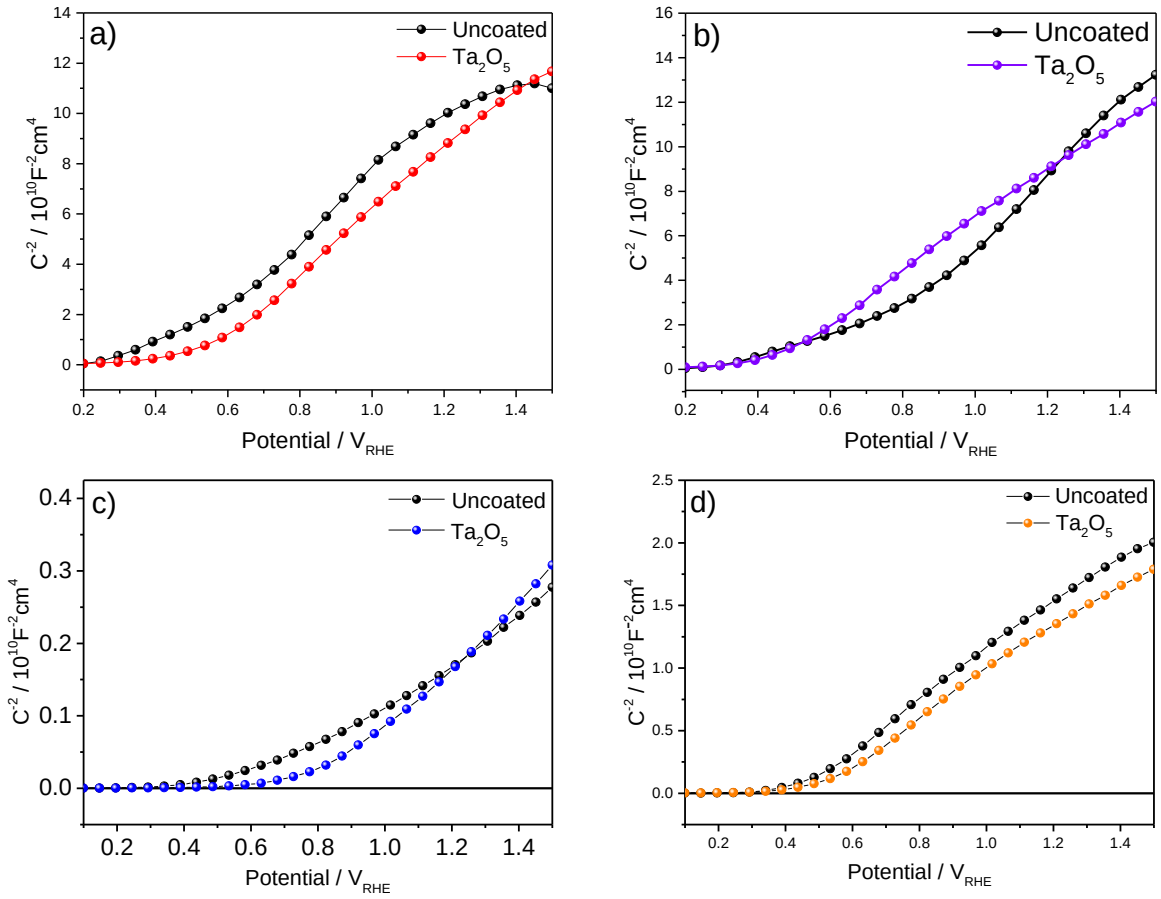

Figure S13. *Mott-Schottky plots of a) 550-Fe_2O_3, b) 750-Fe_2O_3, c) Fe_2O_{3-x} (oxygen deficient) and d) Fe_2O_3 (air annealed), before and after the deposition of a ~2 nm Ta_2O_5 overlayer.*

The donor density can be estimated from the gradient of the Mott-Schottky plot using the relationship in equation 1[6], were *e* is the charge of an electron, ε is the dielectric constant of hematite (80)[7], ε_0 is the permittivity of vacuum (8.854 x10^{-12} F m^{-1}) and *C* is the capacitance derived from the Mott-Schottky plot at each potential.

$$N_d = \left(\frac{2}{e\varepsilon\varepsilon_0}\right)\left[\frac{d\left(1/C^2\right)}{dV}\right]^{-1} \qquad (1)$$

It should be noted that for ideal Mott-Schottky measurements a flat surface is required. A nanostructured surface such as those of the films studied here is expected to cause a significant degree of uncertainty, and as such, we would like to

stress that great caution should be taken when interpreting these measurements. We expect that comparison of two films of the same structure (e.g. the same film before and after Ta_2O_5 deposition) will reduce the associated errors and this method is used to estimate the donor densities of the pairs of films studied here.

Donor densities obtained from Mott-Schottky:

Material	Donor density
550-Fe_2O_3	$1.1x10^{19}$ cm^{-3}
550-Fe_2O_3 / Ta_2O_5	$1.3x10^{19}$ cm^{-3}
750-Fe_2O_3	$1.0x10^{19}$ cm^{-3}
750-Fe_2O_3 / Ta_2O_5	$1.4x10^{19}$ cm^{-3}
Fe_2O_{3-x}	$6.6x10^{20}$ cm^{-3}
Fe_2O_{3-x} / Ta_2O_5	$5.3x10^{20}$ cm^{-3}
Fe_2O_3	$8.6x10^{19}$ cm^{-3}
Fe_2O_3 / Ta_2O_5	$8.8x10^{19}$ cm^{-3}

The small changes in donor densities following the deposition of Ta_2O_5 indicates that an increase in doping is not significant.

1.11 Photocurrent spikes before and after Ta_2O_5 deposition.

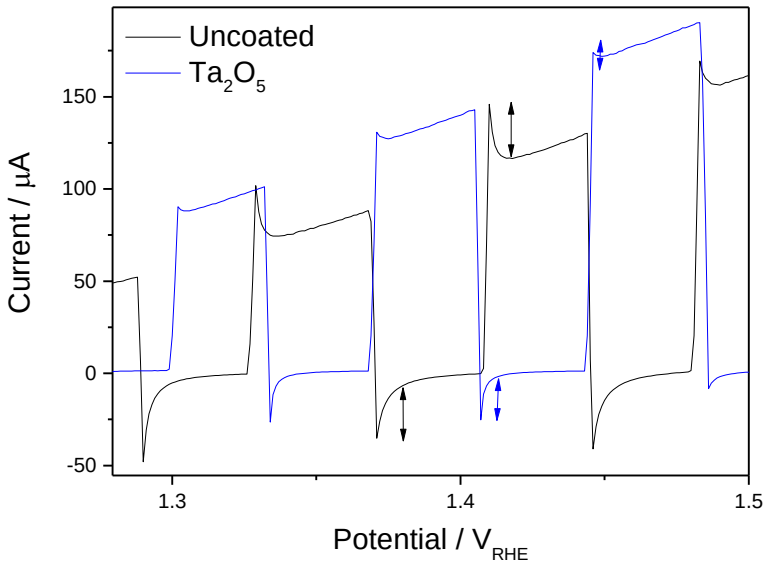

Figure S14. *Close up of chopped photocurrent spikes observed for Fe_2O_{3-x} (oxygen deficient). The spikes appear to be reduced after the deposition of a ~2 nm Ta_2O_5 overlayer. Scans carried out at 10 mV s^{-1} in the dark and under white light illumination (50 mW cm^{-2}).*

1.12 Photocurrent *vs*. time following Ta_2O_5 deposition onto hematite

A slow reduction in photocurrent caused by the addition of Ta_2O_5 is observed over a 12 hour period, decreasing to ca. 50% of the original value.

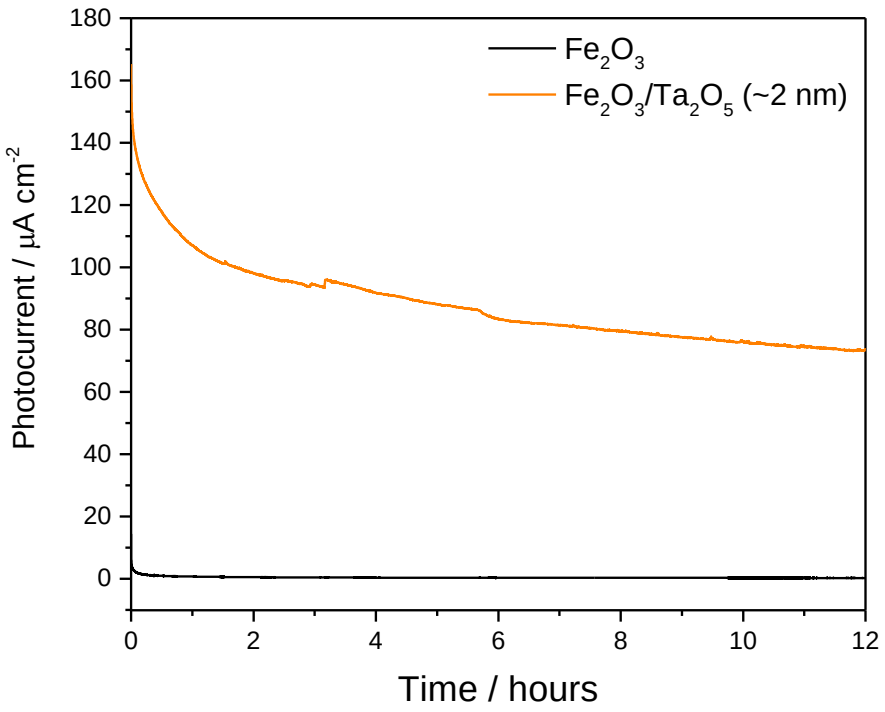

Figure S15. a) *Steady state photocurrent of Fe_2O_3 (black) and Fe_2O_3 with a ~2 nm Ta_2O_5 overlayer (orange), showing that ca. 50% of the photocurrent improvement achieved following ALD remains after 12 hours of continuous illumination. The photocurrents were obtained under white light illumination (50 mW cm^{-2}) and the potential was held at 1.4 V_{RHE} in 1M NaOH electrolyte (pH ~13.7).*

1.13 Linear sweep voltammograms in the dark and under illumination.

Linear sweep photocurrents indicate no significant shift in photocurrent onset potential in any of the films studied here. An anodic shift in the dark electrocatalytic onset potential is observed in all films following the addition of Ta_2O_5 indicating that the surface of the coated films are less catalytic. This may be expected following the deposition of an 'inert, insulating' overlayer.

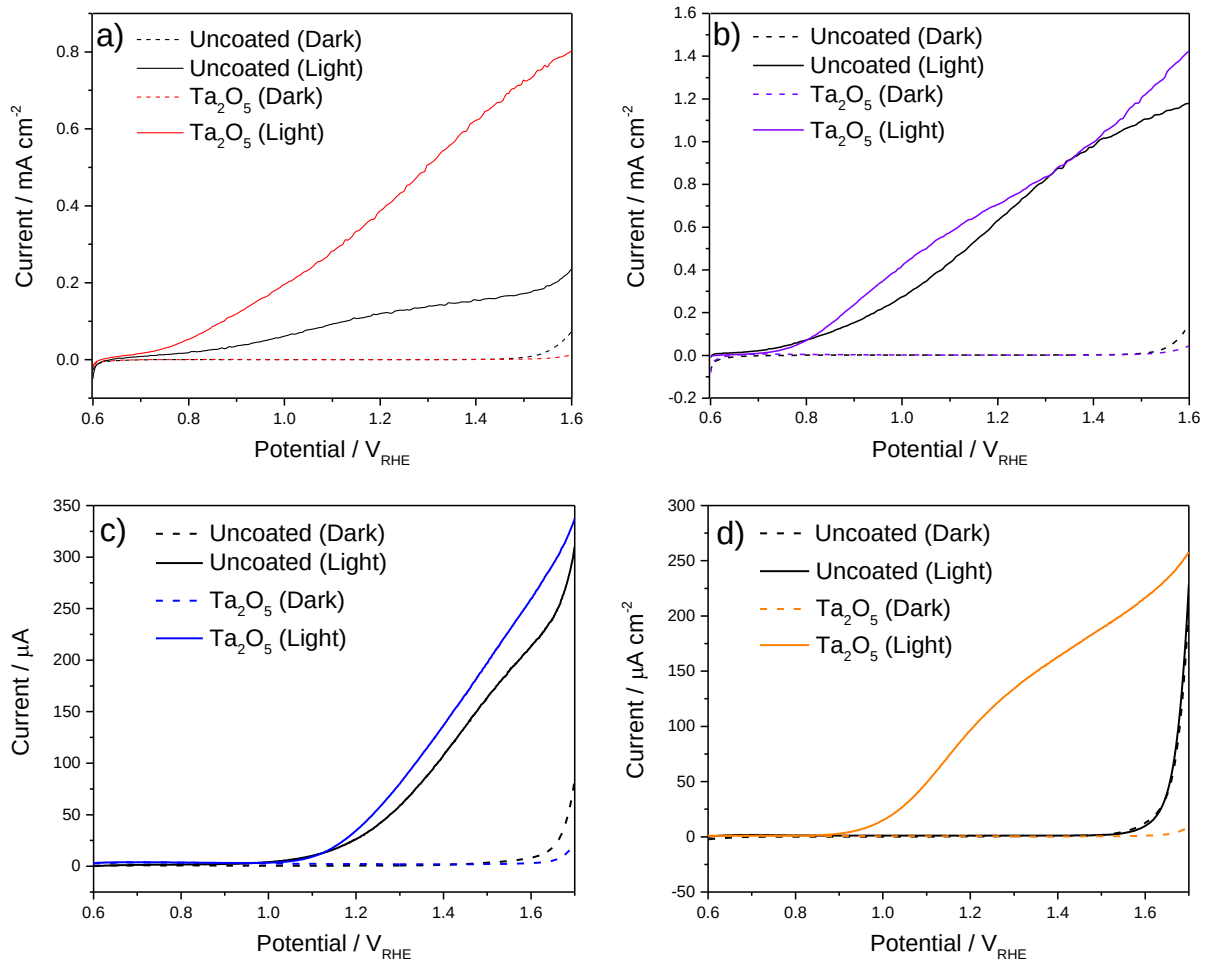

Figure S16. *Linear sweep voltammograms of a) 550-Fe_2O_3, b) 750-Fe_2O_3, c) Fe_2O_{3-x} (oxygen deficient) and d) Fe_2O_3 (air annealed), before and after the deposition of a ~2 nm Ta_2O_5 overlayer. Scans carried out at 10 mV s^{-1} in the dark and under white light illumination (50 mW cm^{-2}).*

1.14 Schematic showing the feature observed by TA spectroscopy which is proposed to be due to photoelectron trapping and de-trapping in hematite.

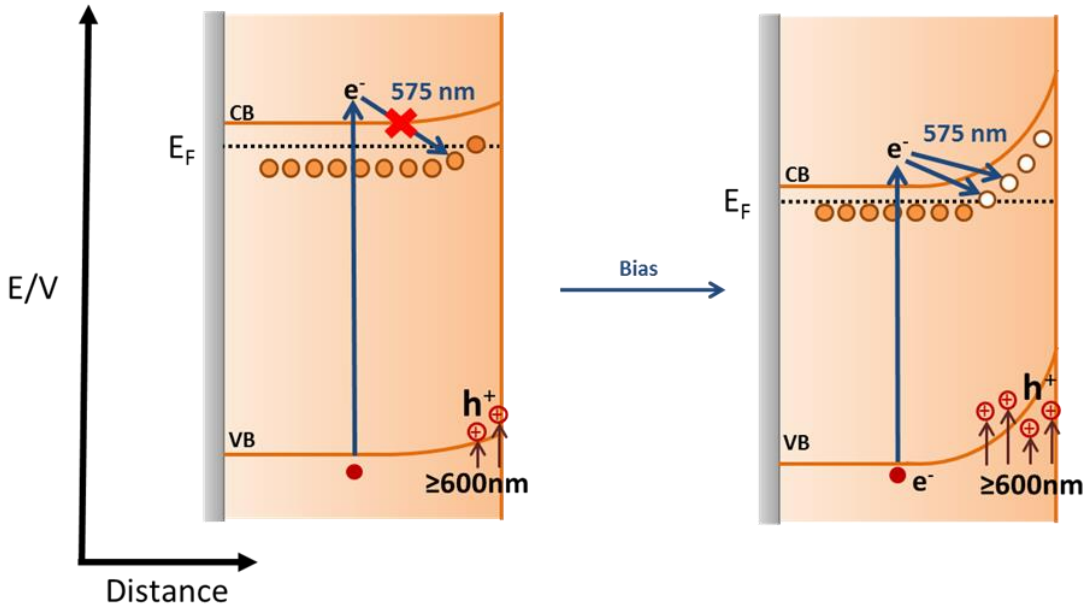

Figure S17. *Schematic showing hematite TAS assignments. The bleach at ~575 nm is observed under a positive bias and is assigned to photo-electron trapping at localised states which is primarily occurring on the sub-microsecond timescale, in line with Barroso et al.*[8]

1.15 Oxygen deficient hematite (Fe_2O_{3-x})

Fe_2O_{3-x} has previously been reported in the literature which demonstrated a simple and effective method for the preparation of highly photoactive hematite for use in PEC water oxidation, without the need for dopants, and at a relatively low activation temperature.[6] Thermal treatment of akaganeite nanowire arrays in an oxygen-deficient environment at 550 ^{O}C resulted in significantly improved photoactivity for water oxidation, as compared to samples that were thermally activated in air. The enhancement in photoactivity is due to an increased donor density resulting from the formation of V_O (Fe^{2+}) and the blocking of back electron recombination[9]. The presence of chloride ions and an oxygen-deficient environment are essential for the creation of V_O.

1.16 Open circuit potential (OCP) measurements

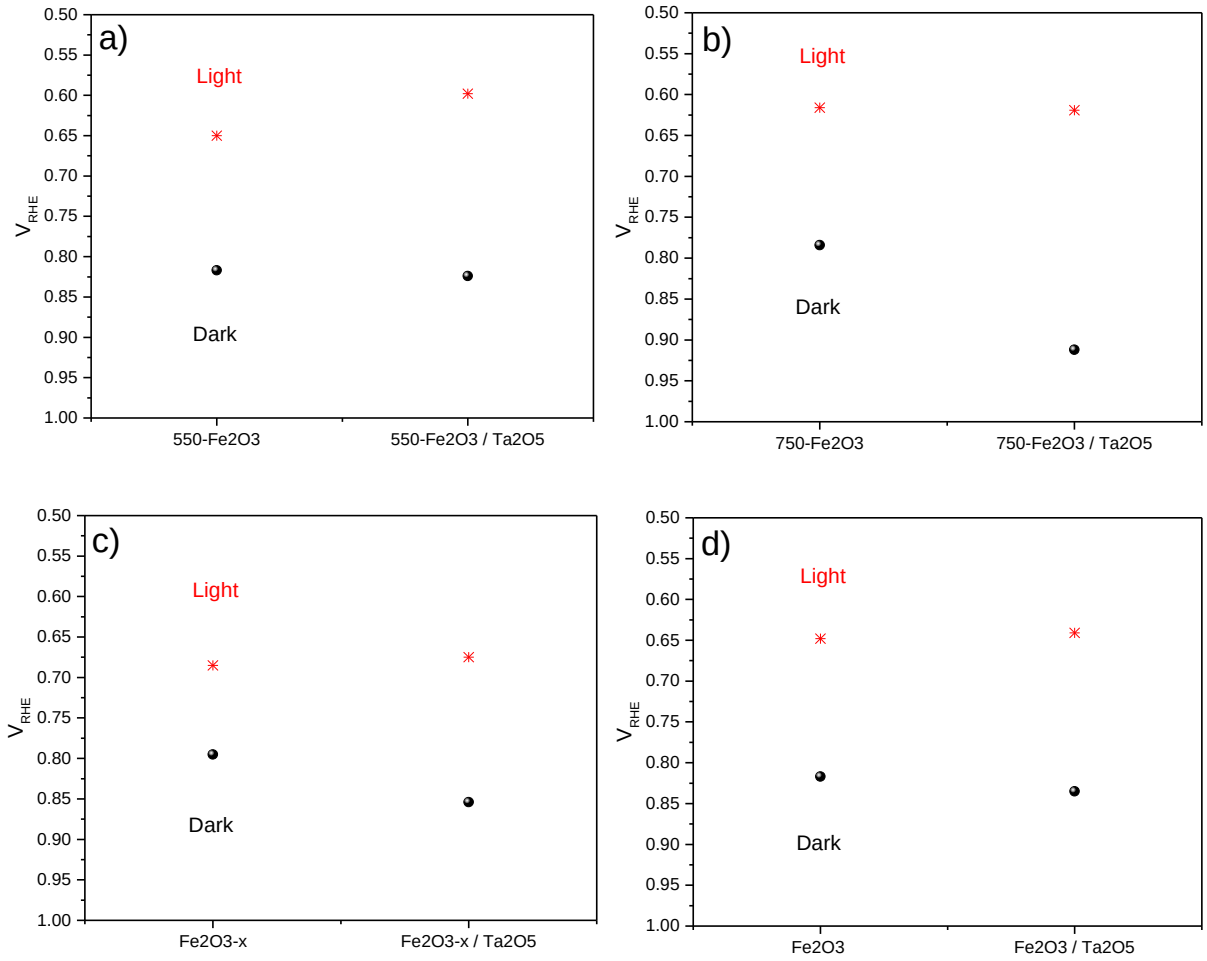

Figure S18. *OCP measurements carried out in the dark (black spheres) and under ca. 50 mW cm^{-2} white light illumination (red stars) for a) 550-Fe_2O_3, b) 750-Fe_2O_3, c) Fe_2O_{3-x} and d) Fe_2O_3 before and after deposition of 2 nm of Ta_2O_5. Samples were left to equilibrate for 20 minutes in order to obtain approximate steady state potentials in either the light or the dark. Potentials under illumination provide a reference point to understand the PEC behaviours, while potentials in the dark can allow observation of removal of Fermi level pinning.*[10]

2 References

[1] H. Wang, J. a. Turner, *J. Electrochem. Soc.* **2010**, *157*, F173.

[2] E. O. Filatova, A. S. Konashuk, *J. Phys. Chem. C* **2015**, *119*, 20755–20761.

[3] W. Chen, Y. Wu, J. Liu, C. Qin, X. Yang, A. Islam, Y.-B. Cheng, L. Han, *Energy Environ. Sci.* **2015**, *8*, 629–640.

[4] W.-J. Chun, A. Ishikawa, H. Fujisawa, T. Takata, J. N. Kondo, M. Hara, M. Kawai, Y. Matsumoto, K. Domen, *J. Phys. Chem. B* **2003**, *107*, 1798–1803.

[5] S. Chen, L. Wang, *Chem. Mater.* **2012**, *3666*, 1–5.

[6] Y. Ling, G. Wang, J. Reddy, C. Wang, J. Z. Zhang, Y. Li, *Angew. Chem. Int. Ed. Engl.* **2012**, *51*, 4074–9.

[7] I. Cesar, K. Sivula, A. Kay, R. Zboril, M. Grätzel, *J. Phys. Chem. C* **2009**, *113*, 772–782.

[8] M. Barroso, S. R. Pendlebury, A. J. Cowan, J. R. Durrant, *Chem. Sci.* **2013**, *4*, 2724.

[9] M. Forster, R. J. Potter, Y. Ling, Y. Yang, D. R. Klug, Y. Li, A. J. Cowan, *Chem. Sci.* **2015**, *6*, 4009–4016.

[10] J.-W. Jang, C. Du, Y. Ye, Y. Lin, X. Yao, J. Thorne, E. Liu, G. McMahon, J. Zhu, A. Javey, et al., *Nat. Commun.* **2015**, *6*, 7447.